Estimating Greenhouse Gas Emissions from Hydrogen-Blended Natural Gas Networks

energies

MDPI

Article

Estimating Greenhouse Gas Emissions from Hydrogen-Blended Natural Gas Networks

Roberto Paglini [1,2,*], Francesco Demetrio Minuto [1,2] and Andrea Lanzini [1,2]

[1] Energy Center Lab, Polytechnic of Turin, Via Paolo Borsellino 38/16, 10152 Turin, Italy; francesco.minuto@polito.it (F.D.M.); andrea.lanzini@polito.it (A.L.)
[2] Department of Energy (DENERG), Polytechnic of Turin, Corso Duca degli Abruzzi 24, 10129 Turin, Italy
* Correspondence: roberto.paglini@polito.it

Abstract: Methane is a significant contributor to anthropogenic greenhouse gas emissions. Blending hydrogen with natural gas in existing networks presents a promising strategy to reduce these emissions and support the transition to a carbon-neutral energy system. However, hydrogen's potential for atmospheric release raises safety and environmental concerns, necessitating an assessment of its impact on methane emissions and leakage behavior. This study introduces a methodology for estimating how fugitive emissions change when a natural gas network is shifted to a 10% hydrogen blend by combining analytical flowrate models with data from sampled leaks across a natural gas network. The methodology involves developing conversion factors based on existing methane emission rates to predict corresponding hydrogen emissions across different sections of the network, including mainlines, service lines, and facilities. Our findings reveal that while the overall volumetric emission rates increase by 5.67% on the mainlines and 3.04% on the service lines, primarily due to hydrogen's lower density, methane emissions decrease by 5.95% on the mainlines and 8.28% on the service lines. However, when considering the impact of a 10% hydrogen blend on the Global Warming Potential, the net reduction in greenhouse gas emissions is 5.37% for the mainlines and 7.72% for the service lines. This work bridges the gap between research on hydrogen leakage and network readiness, which traditionally focuses on safety, and environmental sustainability studies on methane emission.

Keywords: hydrogen emissions; hydrogen blends; hydrogen–methane blending; gaseous fuel leakage; natural gas pipeline; greenhouse gas emissions

Citation: Paglini, R.; Minuto, F.D.; Lanzini, A. Estimating Greenhouse Gas Emissions from Hydrogen-Blended Natural Gas Networks. *Energies* **2024**, *17*, 6369. https://doi.org/10.3390/en17246369

Received: 24 September 2024
Revised: 6 December 2024
Accepted: 11 December 2024
Published: 18 December 2024

1. Introduction

Methane (CH_4) is a potent greenhouse gas, significantly more effective at trapping heat radiation than carbon dioxide (CO_2), especially over a short time frame. According to the IPCC's Fifth Assessment Report, it has a global warming potential of 80 in a 20-year period, decreasing to about 28 over a 100-year period [1]. As the second-largest contributor to anthropogenic greenhouse gas emissions, methane's impact on climate change is substantial.

Anthropogenic methane emissions originate from several human activities and supply chains, such as farming, agriculture, and anaerobic fermentation in sewage systems, and make up biogenic sources of methane emissions. Natural gas production, transport, distribution, and utilization make up fossil sources of methane emissions. Recognizing the urgent need to mitigate these emissions, significant efforts have been dedicated by both academic research and international organizations to the reduction of methane emissions [2–5].

One promising strategy for reducing carbon emissions involves blending sustainable gaseous energy carriers, like hydrogen and biomethane, into existing natural gas infrastructures [6–9]. This approach aims to facilitate low-carbon energy use without requiring extensive new infrastructure. However, hydrogen introduces unique challenges due to its physical properties: it is lighter and has a lower viscosity than methane, which can

influence leakage behavior in gas networks. Moreover, high hydrogen concentrations or a full shift to hydrogen (100% H_2) increases metal embrittlement, potentially altering leak geometry and increasing the frequency of leak events [10–13]. For these reasons, such scenarios often necessitate complete pipeline upgrades using plastic materials instead of metal [14].

Historically, research on hydrogen blending has concentrated on safety and risk analysis, particularly regarding hydrogen leakage. In the early 2000s, several European research initiatives, notably the NaturalHy Project [10,11,15], explored the issue related to end-user exposure to hydrogen leaks [16], the consequences of gas release explosions [17], and assessments of infrastructure durability and integrity [12]. More recent computational fluid dynamic studies have modeled the release and dispersion of hydrogen–methane blends from high-pressure pipelines to evaluate the effect of hydrogen blending on gas concentration fields or plumes and their safety implications [18–20].

While safety considerations are critical, assessing the environmental impacts of hydrogen blending is equally important, especially concerning hydrogen losses. Hydrogen acts as a secondary greenhouse gas by interfering with atmospheric processes that remove primary greenhouse gases [21]. Therefore, to fully evaluate the environmental benefits of blending hydrogen into the natural gas distribution system, it is essential to consider the impact of low-level leaks. These leaks are often significantly smaller than those typically examined in safety and risk analyses but can cumulatively affect greenhouse gas levels [22].

Recent experimental studies have begun to address these environmental considerations. Nohora et al., 2018 [23] and Hormaza et al., 2020 [24] conducted experimental studies on the leakage behavior of methane, hydrogen, and their blends in a low-pressure natural gas distribution system. Their findings indicate that low-pressure leaks from screw threads and fittings did not show a preference for hydrogen and that leakage rates were independent of gas composition. Qin et al., 2024 [25] developed an experimental apparatus to measure leakage rates from loose fittings as well as holes of different geometries on hydrogen system pipelines. Cooper et al., 2022 [26] assessed hydrogen emissions from a hypothetical pure hydrogen scenario in the United Kingdom, considering the entire hydrogen supply chains based on methane emission data and using two flowrate calculation models (laminar flow and free molecular flow, respectively) to convert methane emissions into hydrogen-equivalent values. This methodology bridges the gap between understanding the impact of hydrogen blending on leakage and analyzing current methane emissions from natural gas infrastructures. This connection suggests that existing methane emission data and ongoing leak sampling activities could offer valuable insights into future emissions from hydrogen blends. However, studies on the US natural gas distribution system have highlighted that emission distributions are often not characterized in detail [27–31]. To address this limitation, international organizations, like the United Nations Environmental Program (UNEP) through the Oil and Gas Methane Partnership (OGMP), have developed new leak detection, sampling, and reporting guidelines to enhance the precision of methane emission estimates [4,5].

Analytical models play a crucial role in emission assessments, particularly in calculating leak rates from valves, joints, and sealing components. Early works by Jolly and Marchand [32] and Grine and Bouzid [33] utilized Darcy's Law and Navier–Stokes equations, respectively, to calculate leak rates from gaskets. Subsequent studies by Kazeminia and Bouzid [34,35] investigated the performance of Darcy's model in predicting leak rates from valves and joints under various operating conditions.

These models typically relate the pressure at the leak site to the resulting emission flow rate, with variations based on flow regime and molecular effect. Key parameters, such as the Reynolds number, of whether the flow is laminar or turbulent [36]; the Knudsen number, which indicates whether the fluid can be treated as a continuous body or if rarefaction effects are significant [37]; and the Mach number, distinguishing between subsonic or sonic (choked) flow [38], are fundamental in determining the appropriate model and linking pressure to flow rate. The choice of model depends on factors like pipeline pressure, leak

path geometry, and dimensions, all of which influence both the model selection and the specific equation terms that connect pressure and flow rate [34,35,39].

Conversion factors derived from these models can be used to evaluate the flow rate of a target gas based on the known flow rate of a reference gas. This method has been employed in past studies to estimate hydrogen emission rates using helium as a reference gas for safety implications [40] and infer pure hydrogen emission based on existing methane emission data [26].

Despite advancements in understanding hydrogen leakage and its safety implications, a significant gap remains in quantifying the environmental impact of low-level hydrogen blending on methane and hydrogen emissions within existing natural gas distribution networks.

To address this gap, the present study developed conversion factors for methane–hydrogen blends at a low blending ratio (10%vol.). Utilizing open-source methane leak rate data from a US distribution network [29], we mapped observed methane emissions onto appropriate analytical flow models within the Reynolds–Knudsen–Mach framework. This approach allowed us to estimate how emission rates change with hydrogen blending, providing valuable insights into the environmental consequences of such transitions.

The contributions of this work are as follows:

- Novel methodology: We introduce a method that combines real-world methane emission data with analytical flow models to estimate methane and hydrogen emissions in blended gas networks. This method accounts for various flow regimes and molecular effects, enhancing the accuracy of emission estimations;
- Comprehensive emission assessment: By generating a Blended Emissions Dataset
- Representing methane and hydrogen emissions from leaks across the natural gas distribution network, we provide a tool for quantifying shifts in greenhouse gas emissions due to leakage in blended gas networks compared to pure natural gas networks;
- Policy insights: Our analysis reflects current and developing European policies on hydrogen blending [41], offering valuable insights for policymakers and industry stakeholders regarding the environmental implications of integrating hydrogen into existing gas infrastructures.

2. Materials and Methods

2.1. Methodological Framework

The methodology proposed in this study aims to estimate changes in emission rates for a natural gas distribution network transitioning to a 10% hydrogen–methane blend. This was achieved through a bottom-up approach, calculating emission variations for each individually measured leak across different network subsystems (e.g., mainlines, service lines, and metering and regulation stations) by associating an appropriate analytical flowrate model with each.

At the core of this methodology is the systematic classification of analytical flowrate models within the Knudsen–Reynolds–Mach space, which constitutes our first methodological contribution. These models were categorized based on three key parameters: rarefaction, laminarity, and the sonic nature of the flow. Each model was mapped to its corresponding sub-domain within the Knudsen–Reynolds–Mach space to identify the most suitable analytical model for various leakage conditions. These models were then used to derive a conversion factor, which defined the ratio between natural gas emission rates and hydrogen–methane blend emission rates for specific leakage scenarios.

To apply this methodology, we utilized emission rate measurements from leakage points in a U.S. natural gas distribution network. Each leak was classified into one of four categories based on its emission rate: “Low”, “Medium”, “High”, or “Super”. The classification facilitated the mapping of each leak onto the Knudsen–Reynolds–Mach space to determine the most appropriate analytical model for describing its flowrate.

The conversion factor for each analytical model was subsequently applied to estimate new emission rates under the 10% hydrogen–methane blend scenario. This process was

repeated for all leaks in the dataset, generating the Blended Emissions Dataset, which estimated methane and hydrogen emission rates for the blended scenario. Importantly, the Blended Emissions Dataset preserves the original leak event distribution across the network's subsystems, enabling a direct comparison of emissions between the hydrogen–methane blending scenario and the original natural gas conditions.

A schematic representation of this methodology is shown in Figure 1, illustrating the step-by-step process from emission rate measurement to the generation of the Blended Emissions Dataset.

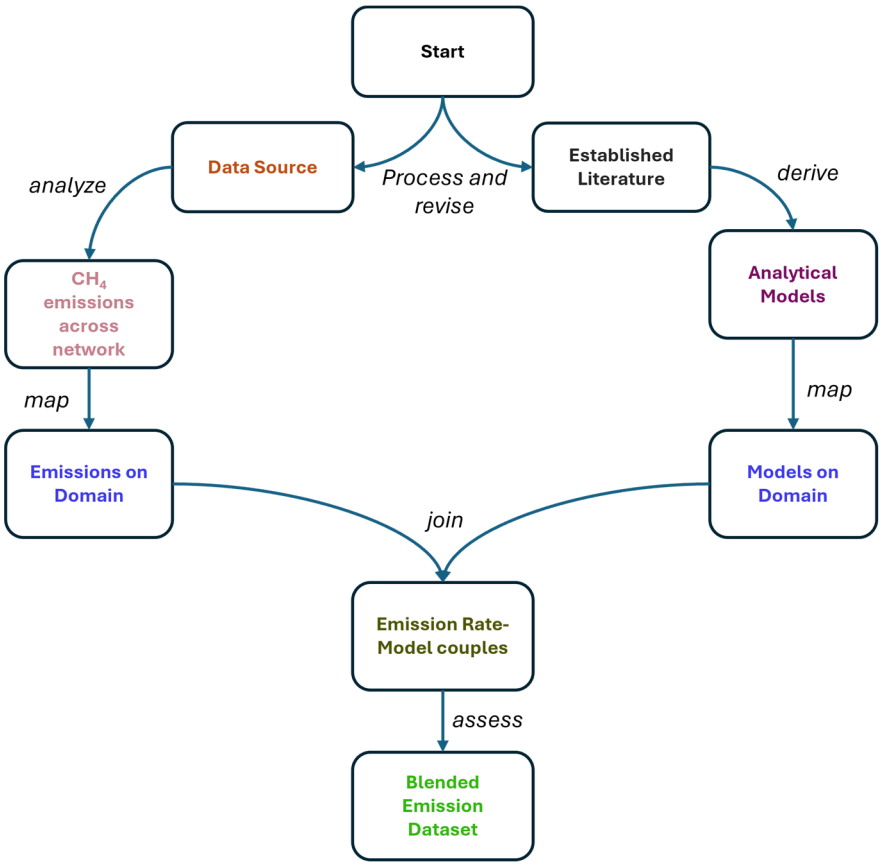

Figure 1. Schematic representation of the steps in this methodology for hydrogen blend emission assessment in fugitive leakage.

2.2. Analytical Flowrate Models

To describe emission rates from different leaks, this study considered a set of established analytical flowrate models. Each model was selected based on the specific characteristics of the flow, determined by key parameters, such as the Reynolds number (Re), Knudsen number (Kn), and Mach number (Ma). The selection criteria for the models are as follows:

- Hagen–Poiseuille Continuous Model (Laminar Continuous Flow Domain): Applicable to low Reynolds, Knudsen, and Mach numbers, where the flow is laminar and slow, and the fluid behaves as a continuous body;
- Hagen–Poiseuille Slip Flow Model (Slip Flow Domain): Relevant for intermediate Knudsen numbers, where molecular interactions between the fluid and the walls become significant, breaking the no-slip condition;
- Free Molecular Diffusion Model (Free Molecular Domain): Used for high Knudsen numbers, where the fluid no longer behaves as a continuous medium and molecular effects dominate the flow;

- Darcy–Weisbach Turbulent-Flow Model and Compressed Gas Release Model (Compressed and Turbulent Domain): Applicable to low Knudsen numbers but high Reynolds and Mach numbers, where turbulence or sonic effects characterize the flow.

The relationship between the Reynolds number, Knudsen number, and Mach number is given by Equation (1):

$$K_N = \sqrt{\frac{\gamma\pi}{2}}\frac{Ma}{Re} \tag{1}$$

where γ is the specific heat ratio. Using this relationship, the flowrate models were mapped onto the Reynolds–Knudsen–Mach (Re-Kn-Ma) space. This mapping identified the specific sub-domain in which each model was valid, enabling precise selection of the appropriate analytical model for various leakage conditions. The resulting mapping is illustrated in Figure 2, providing a clear framework to determine which flowrate model is most suitable for a given emission condition.

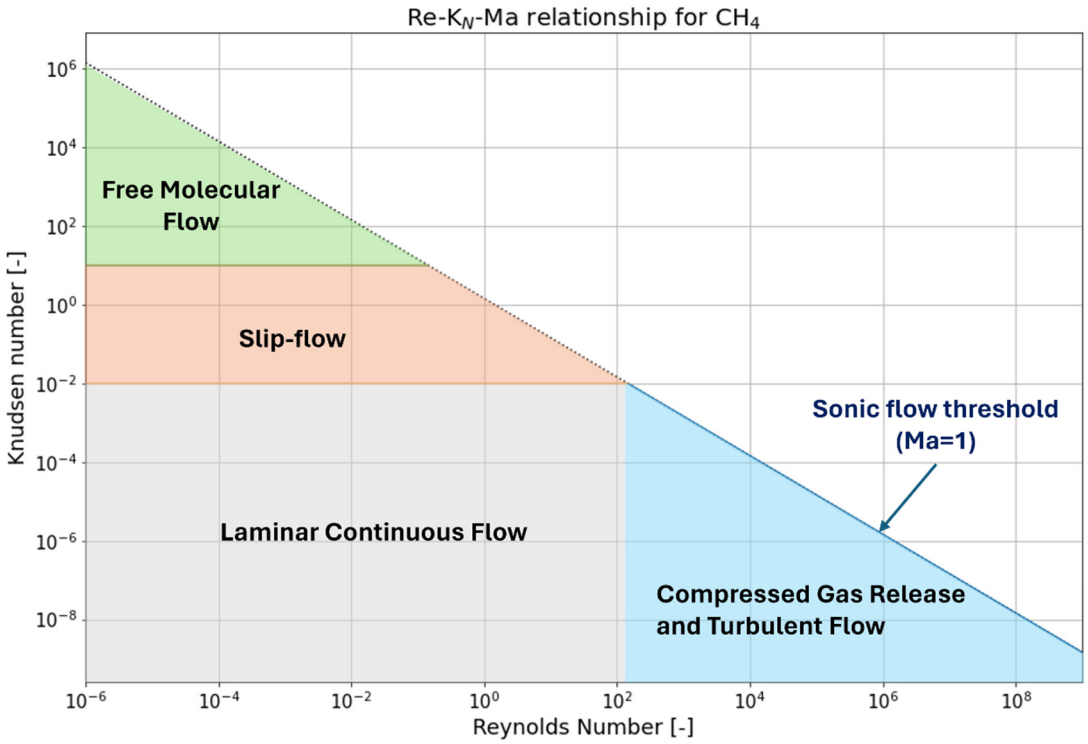

Figure 2. Mapping of the different flowrate moles considered in this study. The figure shows the Re-KN-Ma space and the area of application of the Hagen–Poiseuille continuous model, the slip flow model, and the free molecular flow model at low Reynold's number (turbulence) and closer to the Ma = 1 curve, delimiting the sonic flux.

2.2.1. Laminar Continuous Flow Domain

The Hagen–Poiseuille model provides the analytical solution of the Navier–Stokes equations for a steady-state, laminar flow through a pipeline with a circular and constant cross-section [36], as shown in Equation (2):

$$Q_{Hagen-Poiseuille} = \frac{\pi D^4 \Delta p}{128 \mu L} \tag{2}$$

where Q is the volumetric gas flowrate, D is the hydraulic diameter of the pipeline, Δp is the pressure difference between two points in the pipeline with distance L, and μ is the gas dynamic viscosity. The conversion factor resulting from this model is shown in Equation (3):

$$CF = \frac{\mu_N}{\mu_B} \simeq 1 \tag{3}$$

where μ_N is the dynamic viscosity of natural gas, and μ_B is the dynamic viscosity of the hydrogen–methane blend at a 10%vol. hydrogen blending ratio. At this blending ratio, the viscosity of the hydrogen–methane blend is similar to that of natural gas [42]; thus, the overall conversion factor for the continuous Hagen–Poiseuille model was evaluated as 1.

2.2.2. Slip Flow Domain

The slip flow model is an adjustment of the Hagen–Poiseuille model for flowrates occurring in small channels where rarefaction effects rise and the hypothesis of continuous fluid is not satisfied [43]. This model can be described by Equation (4), and its conversion factor can be described by Equation (5):

$$Q_{slip-flow} = \frac{WH^3 p_e^2 \overline{M}}{24\mu L \overline{R} T \rho} * f(\mathrm{K_N},\ TMAC,\ \beta) \tag{4}$$

$$CF = \frac{\mu_B * f_N}{\mu_N * \mathrm{f_B}} \simeq 1.01 \tag{5}$$

where W is the pipeline width and H is the pipeline height (the formula was originally applied on a rectangular cross-section [39]), p_e is the atmospheric pressure, $\overline{M}$ is the gas molar mass, μ is the gas dynamic viscosity, L is the pipeline length, $\overline{R}$ is the ideal gas constant, ρ is the gas density, T is the temperature, K_N is the Knudsen number, $TMAC$ is the Tangential Momentum Accommodation Coefficient, and β is the pressure ratio.

Understanding the value of $f(\mathrm{K_N},\ TMAC,\ \beta)$ is crucial for properly assessing the conversion factor. The pressure ratio was evaluated considering a pipeline pressure of 1.04 bar, as this value was considered representative of low-pressure equipment in distribution system operators. However, different operators might set different thresholds to define low-pressure infrastructure; thus, this value should be adjusted on a case study basis, considering the specifics of the system under analysis. Supplementary Materials provide a sensitivity analysis for the slip flow correction factor considering different values for the pressure ratio (see Figures S1 and S2 of Supplementary Materials). Regarding the TMAC value, we sourced it from Ge and Sutton's results (2006) [39]. As for the Knudsen number, its value spans from 0.01 to 0.1 within the slip flow regime. The conversion factor values were evaluated at the highest Knudsen number value to be conservative on the gas loss estimate. Therefore, the conversion factor value used in this study for the slip flow Hagen–Poiseuille model is 1.01.

2.2.3. Free Molecular Domain

Free molecular flow is used to describe flow in extremely rarefied conditions typically associated with low pressure or extremely tight gaps. In these conditions, the fluid does not behave as a continuous body any longer, and the molecules move according to Knudsen diffusion [37,44,45], as described in Equation (6):

$$\vec{J_i} = D_{KN,i} * \nabla(p_i) \tag{6}$$

where J_i is the molar flow, $D_{KN,i}$ is the Knudsen Diffusivity, and $\nabla(p_i)$ is the partial pressure gradient. The subscript "i" states the species for which these parameters are evaluated.

In principle, the application of this model could imply the need for knowledge about the partial pressure distribution across the leak path; however, experimental observations show that the mixture composition remains constant if the flow is in free molecular flow conditions [46]. Therefore, it is possible to simplify Equation (6) into Equation (7):

$$\vec{J_{i_{th}}} = D_{KN_{i_{th}}} * c_{i_{th}} \nabla(p) \tag{7}$$

In this form, the free molecular flow depends on the Knudsen diffusion (DKN), the species concentration (c_i), and the pressure gradient across the leak ($\nabla(p)$). As the

Knudsen diffusion depends on the species molecular mass ($\overline{M}$) according to Equation (8), the conversion factor for the leak rate change is described in Equation (9):

$$D_{KN_{i_{th}}} \propto \sqrt{\frac{\overline{R}T}{2\pi\overline{M}_{i_{th}}}} \tag{8}$$

$$CF_{\mathrm{B}}^{CH_4 \to H_2} = \sqrt{\frac{\overline{M}_{CH_4}}{\overline{M}_{H_2}}} = 0.35 \tag{9}$$

where $\overline{M}$ is the molecular mass, $\overline{R}$ is the universal gas constant, and T is the temperature. The subscript "B" and the superscript "$CH_4 \to H_2$" indicate that this conversion factor defines the ratio between hydrogen and methane emission rates from within the same leak of the hydrogen–methane blend. Furthermore, methane conversion is based on Equation (6); the Knudsen diffusion coefficient and the total pressure gradient remain unchanged, whilst the methane concentration is different in natural gas and the blend. Therefore, the conversion factor for methane aims to assess the methane-only leak rate change from natural gas to the blend, as shown in Equation (10):

$$CF_{CH_4}^{\mathrm{N}\to\mathrm{B}} = \frac{C_{\mathrm{CH_4},B}}{C_{\mathrm{CH_4},N}} = \frac{0.81}{0.90} = 0.90 \tag{10}$$

The subscript "CH_4" and superscript "N → B" indicate that this conversion factor defines the ratio between the methane emission rate of the same leak considering the methane fraction of the hydrogen–methane blend and the methane fraction of natural gas.

2.2.4. Compressed and Turbulent Domain

The turbulent-flow model is described by Equation (11), and the resulting conversion factor is shown in Equation (12):

$$Q = 0.354\pi * \frac{D^{2.5}\sqrt{\Delta p}}{\sqrt{fL\rho}} \tag{11}$$

$$CF = \sqrt{\frac{\rho_N}{\rho_{\mathrm{B}}}} \tag{12}$$

where D is the leak hydraulic diameter, Δp is the pressure difference between the pipeline and external environment, f is the friction factor, and ρ is the gas density. The conversion factor resulting from this model is 1.05.

The compressed gas release model is often used in safety and risk analysis to estimate gas losses from pressurized vessels [38]. This model results from the application of nozzle theory, where the flowrate calculation is derived from the energy balance of an adiabatic expansion of gas, as shown in Equation (13):

$$Q = \left\{ \frac{2\gamma}{\gamma - 1} * \frac{p_0}{\rho_0} * \left(\frac{p_{env}}{p_0}\right)^{\frac{2}{\gamma}} * \left[1 - \left(\frac{p_{env}}{p0}\right)^{\frac{\gamma-1}{\gamma}}\right] \right\}^{0.5} \tag{13}$$

where γ is the adiabatic expansion coefficient, $p0$ and $\rho 0$ are the gas pressure and density inside the vessel, and p_{env} is the atmospheric pressure. The conversion factor associated with this model was defined, as shown in Equation (14):

$$CF = \sqrt{\frac{\overline{M}_{CH_4}}{\overline{M}_{H_2}}} * \frac{g(\gamma_{H_2})}{g(\gamma_{CH_4})} \simeq 1.05 \tag{14}$$

where $\overline{M}_{CH4}$ and $\overline{M}_{H2}$ are the molar masses of methane and hydrogen, and $g(\gamma)$ represents the part of the function that depends on the adiabatic exponent.

2.3. Flowrate Conversion Factors

To estimate emission rates from hydrogen–methane blends, measured flow rates from natural gas fugitive emissions are converted using a conversion factor, as shown in Equation (15):

$$Q_B = CF * Q_N \quad (15)$$

where Q_B is the calculated volumetric emission rate of blended gas, Q_N is the measured volumetric emission rate of natural gas, and CF is the conversion factor. Throughout this study, the subscript "N" refers to properties or flowrates of natural gas, while "B" refers to the hydrogen–methane blend.

The conversion factor (CF) is defined as the flowrate ratio between two gases, as introduced by Schefer et al. [40]. This concept has been extended in this study to additional flow regimes, including slip flow and free molecular flow, and applied to gas mixtures rather than pure gases alone.

This approach assumes that the leak geometry and operative pressure of pipelines are not correlated to gas composition. This assumption generally holds for low hydrogen blending ratios, while higher blending ratios require adjustments in operating pressure to maintain energy flow due to hydrogen's lower volumetric energy density. Moreover, a higher blending ratio should account for the effect of hydrogen embrittlement in metallic pipelines, which will likely result in an increase in the number of leak events or changes in the leak geometry.

In this study, we considered a relatively low hydrogen blending ratio of 10% by volume, where the effects on leak geometry and operating pressure were assumed negligible.

The compositions of natural gas and the hydrogen–methane blend used in this study are summarized in Table 1. Natural gas was approximated as 90% methane and 10% other gases, while the blend was approximated as 81% methane, 10% hydrogen, and 9% other gases, maintaining the methane-to-other-gases ratio.

Table 1. Natural gas and blend reference compositions in this study.

Gas Mixture	Reference Subscript	CH4 (%vol.)	H2 (%vol.)	Other Gases (%vol.)	Methane-to-Other-Gases Ratio (-)
Natural Gas	N	90	0	10	9:1
Blend Gas	B	81	10	9	9:1

In both the Laminar Continuous Flow domain and the slip flow domain, gas mixtures are treated as average gases with composition-averaged properties. In the free molecular flow domain, where the continuity assumption no longer holds, methane and hydrogen are treated as separate components within a binary mixture, as described in the following equations:

$$Q_{CH_4,\,B} = CF_{CH_4} * Q_{CH_4,\,N} \quad (16)$$

$$Q_{H_2,\,B} = CF_{H_2} * Q_{CH_4,\ N} \quad (17)$$

All the conversion factors presented are summarized in Table 2.

Additionally, Table 3 shows the gas species-specific conversion factors defined by the ratio between the target gas (either CH_4 emissions from a blend or H_2 emissions from a blend) and the reference gas (CH_4 emissions from natural gas).

Table 2. Conversion factors associated with each flowrate model. For all models but the free molecular flow one, the continuous hypothesis holds; thus, the conversion factor has one value for the entire natural gas flow. Conversely, for the free molecular flow model, two values are provided: one specific for the methane molecules and one specific for the hydrogen ones.

Flowrate Domains	Conversion Factor	Converting From	Converting To	Continuous Hypothesis
Laminar Continuous Flow	1.00	Natural Gas	H_2/CH_4 Blend	Applicable
Slip Flow	1.01	Natural Gas	H_2/CH_4 Blend	Applicable with Slip-Boundary Condition
Compressed and Turbulent Domain	1.05	Natural Gas	H_2/CH_4 Blend	Applicable
Free Molecular Flow	0.90	CH_4 in Natural Gas	CH_4 in Blend	Not Applicable
	0.35	CH_4 in Blend	H_2 in Blend	Not Applicable

Table 3. Gas species-specific conversion factors are defined as ratio between target gas (CH_4 or H_2 in blend) and reference gas (CH_4 in natural gas).

Flowrate Domains	Gas Species	Conversion Factor	From Gas	To Gas	Continuous Hypothesis
Laminar Continuous Flow	CH_4	0.90	CH_4 in Natural Gas	CH_4 in Blend	Applicable
	H_2	0.11		H_2 in Blend	
Slip Flow	CH_4	0.91		CH_4 in Blend	Applicable with Slip-Boundary Condition
	H_2	0.11		H_2 in Blend	
Compressed and Turbulent Domain	CH_4	0.95		CH_4 in Blend	Applicable
	H_2	0.12		H_2 in Blend	
Free Molecular Flow	CH_4	0.90		CH_4 in Blend	Not Applicable
	H_2	0.32		H_2 in Blend	Not Applicable

2.4. Data Source and Classification

The emission rate data used in this study were obtained from the sampling conducted by Lamb et al., 2015 on an American natural gas distribution network [29] (data available at https://doi.org/10.1021/es505116p, (accessed on 18 July 2024); see Appendices C and E in Supplementary Materials). These data, collected from over 800 leaks sampled in 2013 and 2014, include detailed information as follows:

Pipeline subsystem type: location of the leak (e.g., mainlines, service lines, pressure reduction units, and metering and regulation stations);

- Emission rate measurement: based on a high-flow sampling experiment;
- Pipeline material: for mainlines and service lines, including cast iron, protected and unprotected steel, and plastic;
- Leaking component: for facilities, such as valves, connectors, and other related equipment.
- The key information contained in the dataset is summarized in Table 4.

The emission distribution for pipelines is shown in Figure 3 to provide additional insights into the data characteristics. The curve represents a lognormal function fitted on the sampled emission rate values present in the original data source. The fitting process yields to the following parameters:

- The mean value of the associated normal distribution is −1.39 (scale parameter: 0.25);
- The standard deviation of the associated normal distribution is 1.80 (shape parameter).

This skewed shape is typical for emission distributions of oil and gas leaks [27,29]. The skewness means that a small portion of emissions is associated with high emission rates, thus, the majority of the network's gas losses, whereas the vast majority of leaks have relatively low emission rate values [31,47].

Table 4. Original dataset key information.

Pipeline/Facility Type	Material	Number of Leaks in Dataset
Mains	Unprotected Steel	74
	Protected Steel	32
	Plastic	23
	Cast Iron	13
	Unknown	5
Services	Plastic	38
	Unprotected Steel	19
	Protected Steel	12
	Unknown	7
	Cast Iron	3
TDTS—Distribution	Information Not Included in Dataset	271
Regulating		202
TDTS—Transmission		140
Metering and Regulating		69
Vault		11

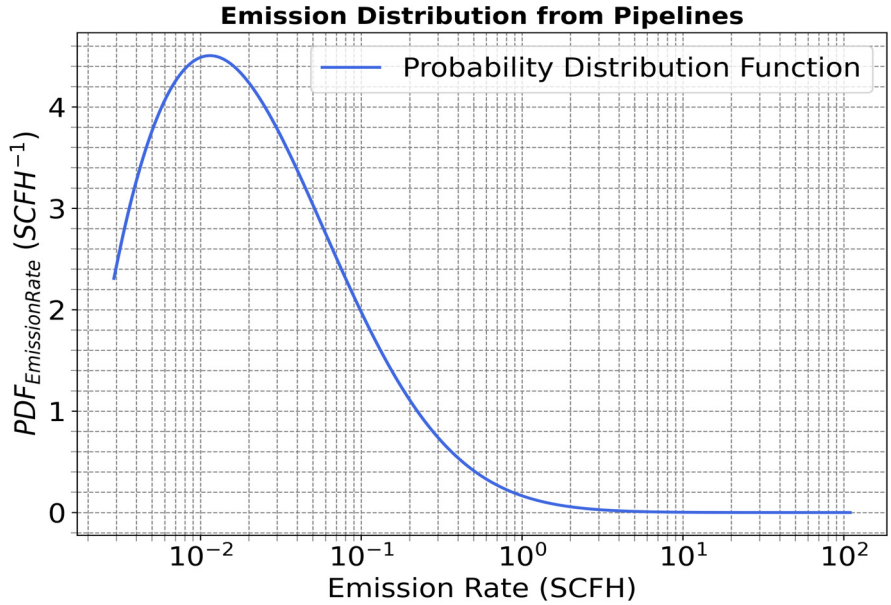

Figure 3. Emission distribution for mainlines and service lines resulting from a lognormal fit on the sample. The emission distribution is skewed, meaning that a small portion of emission rates is significantly higher than the mode.

Once the conversion factors were evaluated for each model, it was necessary to associate each methane leak in the dataset to a model in order to evaluate the new flowrate that would result from blending hydrogen in the network. Therefore, leaks were binned based on the emission rate size according to a similar logic in existing studies [48,49]. Leaks with an emission rate below 0.1 SCFH were classified as "Low", leaks between 0.1 and 2 SCFH were classified as "Medium", leaks between 2 and 10 SCFH were classified as "High", and those above 10 SCFH were classified as "Super". "Low" and "Medium" emission rates were associated with the two Hagen–Poiseuille models: "Low" emissions were associated with the slip flow boundary condition, whilst the "Medium" emissions were associated with the continuous flow model. The reasons behind this choice lie in the following facts: first, the equivalent leak diameter of the Hagen–Poiseuille models (calculated for these emission rates and pipeline pressures) appeared significantly lower than 1mm; thus, it was compliant with the modeling of leakage from loose threads rather than macroscopic holes. Moreover, the lower emission rates were likely associated with

smaller gaps and, thus, higher Knudsen number values. Conversely, "High" and "Super" emissions were associated with the Compressed Gas Release model and the turbulent Darcy–Weisbach model, respectively, as these models yielded equivalent leak diameters of sizes similar to 1mm, which were coherent with macroscopic holes on component surfaces. These association criteria are summarized in Table 5.

Table 5. Emission binning and associations with analytical models.

Emission Rate (x)	Emission BIN	Analytical Model	Conversion Factor	Reasoning
x < 0.1 SCFH	Low	Hagen–Poiseuille Slip Flow	1.01	$D_{eq\ leak} \ll 1$ mm
0.1 < x < 2.0 SCFH	Medium	Hagen–Poiseuille Continuous Flow	1.00	$D_{eq\ leak} \ll 1$ mm
2 < x < 10.0 SCFH	High	Compressed Gas Release	1.05	$D_{eq\ leak} \sim 1$ mm
x > 10.0 SCFH	Super	Darcy–Weisbach Turbulent Flow	1.05	$D_{eq\ leak} \sim 1$ mm

The natural gas emission data obtained from field measurements using the Hi-Flow Sampler in Lamb et al. [29] were classified into "Low", "Medium", "High", and "Super" categories based on the directly measured emission rate value. Then, each emission in the dataset was mapped to the appropriate flow models per the association criteria mentioned above. Figure 4 displays the results of this classification process on the emissions from pipelines. Reflecting the emission rate distribution, the Hagen–Poiseuille continuous flow is the most frequent one for pipeline emissions (57% of sample emissions), followed by the Hagen–Poiseuille slip flow model (29%) and, finally, the Compressed Gas Release model (12%) and the turbulent-flow Darcy–Weisbach model (2%).

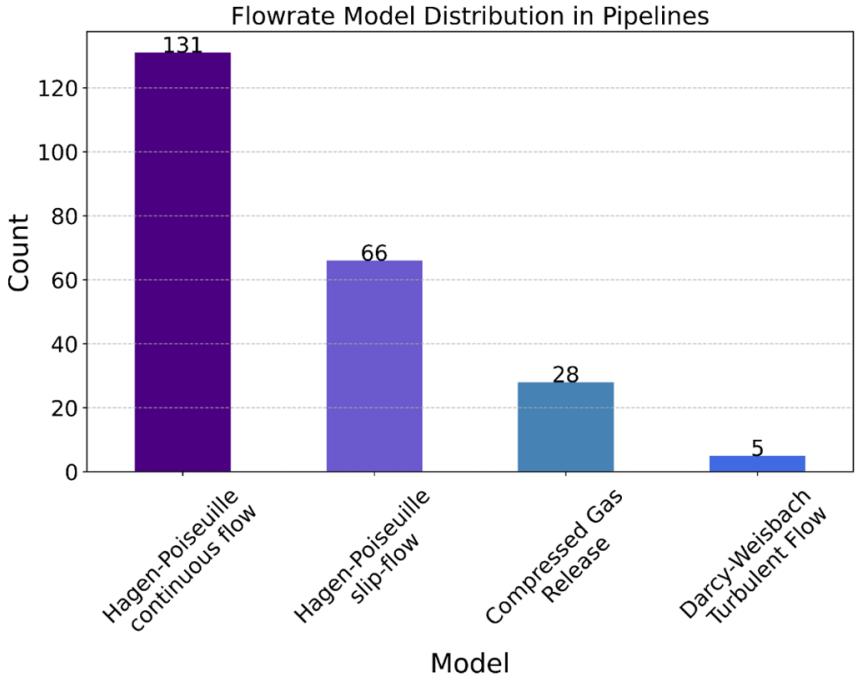

Figure 4. Analytical model distribution in pipelines.

Figure 5 displays the results of the classification process on emissions from the facilities. These emissions appear dominated by the high occurrence of the Hagen–Poiseuille slip flow model (52% of the total leaks from metering and regulation stations). The Hagen–Poiseuille continuous model remains relevant (38%). Finally, the Compressed Gas Release (7%) and the turbulent-flow Darcy–Weisbach (3%) models represent the heavy tail of emissions.

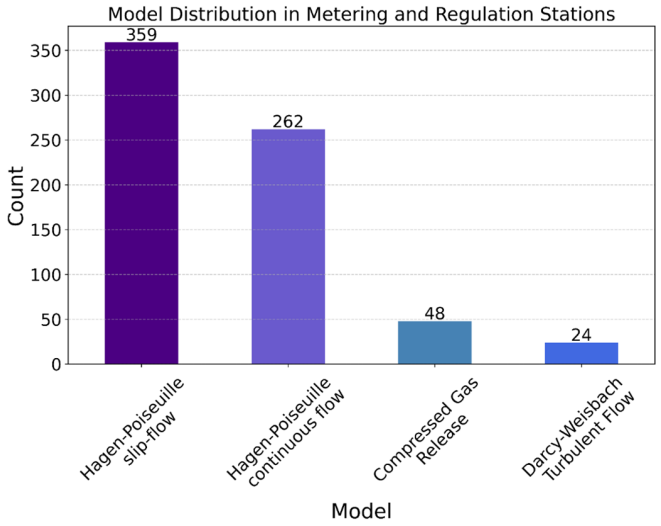

Figure 5. Model distribution in metering and regulation stations.

The free molecular flow model was not applied to any of the leaks in this study as it is specifically designed for leaks occurring under extremely rarefied conditions, such as low pressure or very tight gaps. Such leaks are expected to be significantly smaller than those identified using the Hi-Flow Sampler [29]. Moreover, since the original data source does not provide a detailed description of the leaking components and their causes, the authors did not have sufficient grounds to select this model.

3. Results

3.1. CH_4 and H_2 Emission Rate Change Estimates

The following paragraph describes the results of the emission rate conversion based on the methodology described above. Figure 6 illustrates the distribution of the mean emission rates of methane and hydrogen calculated for the mainlines and service lines. The total (summed) emission rate of methane and hydrogen appears higher than the original methane loss, with a rise of 5.67% for the mainlines and 3.04% for the service lines. This increase is primarily attributed to the low-density hydrogen contributing to the new emissions. It is important to note that while the total emission rate increases, the methane emission rates are consistently lower in the blending scenario than in the original one. Specifically, methane emissions were reduced by 5.95% for the mainlines and 8.28% for the service lines.

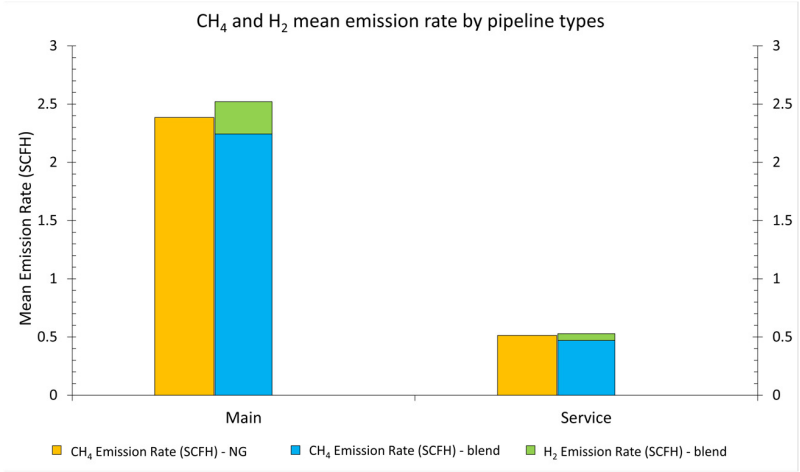

Figure 6. Mean emission rates from natural gas and blend losses from mainlines and service lines. Results are stacked by species (methane and hydrogen).

The numerical values of the emission rates are reported in the upper rows in Table 6, offering a detailed comparison of the emission rates before and after the blending process.

Table 6. Methane and hydrogen mean emission rates per leak event from natural gas and blend.

Emission Location	Mean CH_4 Emission Rate (NG) [SCFH]	Calculated Mean CH_4 Emission Rate (Blend) [SCFH]	Calculated Mean H_2 Emission Rate (Blend) [SCFH]
	Pipeline Type		
Mains	2.38	2.24	0.28
Service Lines	0.51	0.47	0.06
	Pipeline Type and Material		
Mains—Unprotected Steel	2.35	2.21	0.27
Mains—Protected Steel	3.48	3.28	0.40
Mains—Cast Iron	2.64	2.48	0.31
Mains—Plastic	0.83	0.77	0.10
Services—Unprotected Steel	1.01	0.94	0.12
Services—Protected Steel	0.45	0.42	0.05
Services—Cast Iron	0.18	0.16	0.02
Services—Plastic	0.38	0.34	0.04
	Facility Type		
TDTS—Transmission	2.29	2.16	0.27
Metering and Regulating	1.67	1.57	0.19
TDTS—Distribution	1.40	1.31	0.16
Regulating	0.87	0.81	0.10
Vault	0.073	0.066	0.009

It was also possible to evaluate the new mean emissions by material, as this information was present in the original data source. Figure 7 shows the results by pipeline material: the emission rate increase was 5.5% for unprotected steel, 5.7% for cast iron, 3.2% for plastic pipelines, and 5.8% for cathodically protected steel. The methane emission rates were reduced as a consequence of hydrogen blending: 6.1% for unprotected steel, 5.9% for cast iron, 8.1% for plastic pipelines, and 5.8% for protected steel. Table 6 provides a more detailed representation of these results by showing the mean emission rates broken down by pipeline type and material.

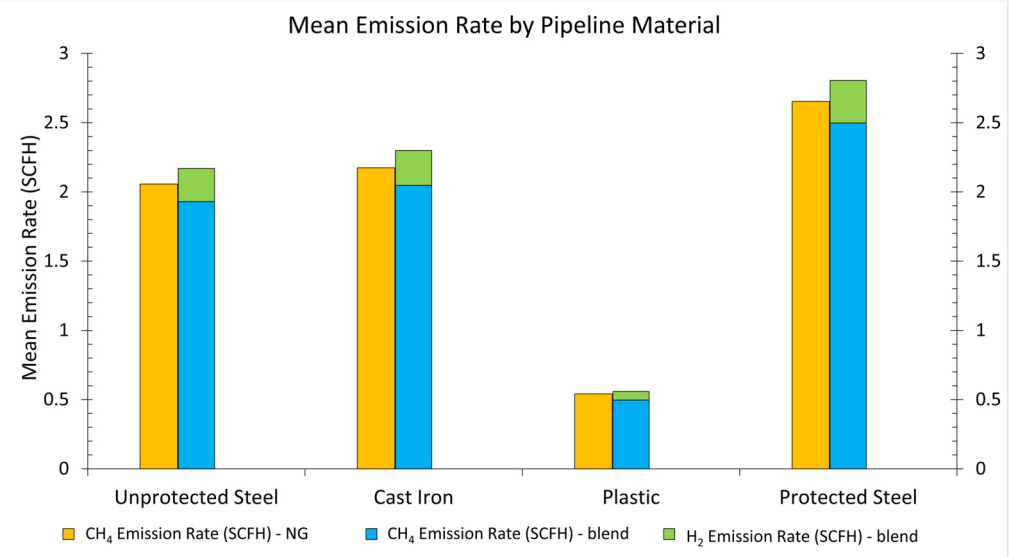

Figure 7. Mean emission rates from natural gas and blend losses from pipelines composed of different materials. Results are stacked by species (methane and hydrogen).

Finally, Figure 8 shows the results for the main facility types: transmission distribution transition stations (TDTSs), metering and regulation stations, regulating stations, and vaulted facilities. The emission rate increase was 5.6% for the transmission end of the transition stations (TDTS—Transmission), 5.5% for the metering and regulating stations, 5.5% for the distribution end of transition stations (TDTS—Distribution), 5.2% for regulating stations, and 1.5% for vaulted facilities. However, due to the presence of hydrogen in the fugitive blend, the methane emission rate was lower than the original emission rate. Methane emissions decreased by 6.1% for TDTS—Transmission, metering and regulating stations, and TDTS—Distribution; 6.4% for regulating stations; and 9.6% for vaulted facilities.

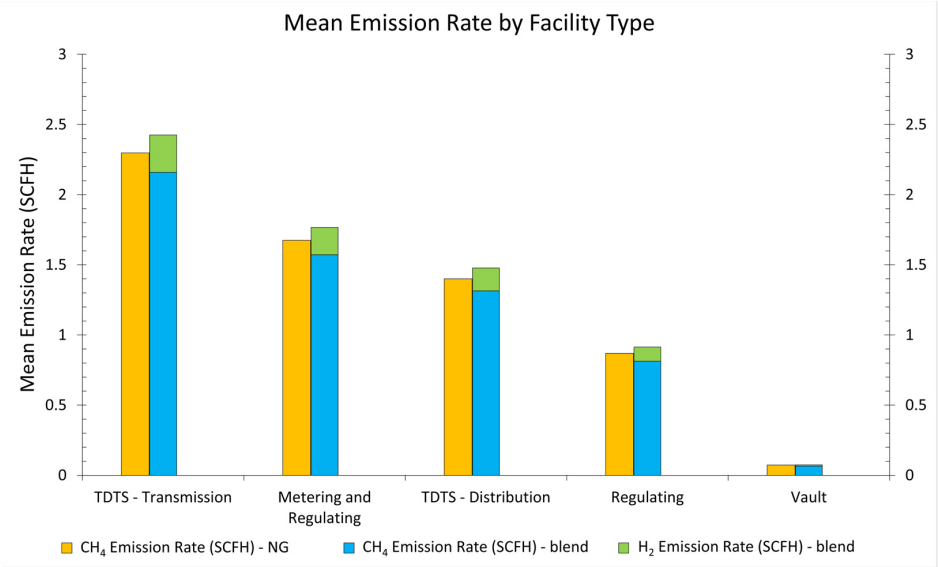

Figure 8. Mean emission rates from natural gas and blend losses from facilities. Results are stacked by species (methane and hydrogen).

The numerical values of the mean CH4 and H2 emission rates from natural gas and the blend are shown in the bottom rows in Table 6. Moreover, a detailed breakdown of the mean emission rates for each component type reported in the original data source is provided in Supplementary Materials.

These results show that the presence of hydrogen in the leaking gas tends to increase the total mean emission rate per leak event for all emission locations. However, cast iron and plastic service lines display similar mean emission rates per leak event (0.18 and 0.38 SCFH, respectively, summing CH_4 and H_2 in the blending scenario) in both scenarios. This observation aligns with the experimental results in Ref. [24] for low-pressure pipeline leakage, which is a realistic operative condition for service lines as they are located in close proximity to end-users and are directly connected to customer meters. The empirical results from Ref. [50] on hydrogen–methane blends for underground pipeline leakages appear higher than our mean emission rates per leak event (7–10 $\times$ 10^3 SCFH of total leaking flowrate). However, this apparent discrepancy is already present in the original data source from Ref. [29], in which the maximum emission rate measured from the underground mainline was 1.09 $\times$ 10^2 SCFH, and the majority of the measurements were in the 10^0 SCFH order of magnitude. Therefore, this discrepancy might depend on the fact that the experiment in Ref. [50] was focused on a specific high-pressure leakage from underground pipelines, whilst this study addresses the mean emission rates for the entire leakage distribution.

3.2. Greenhouse Gas Emission Change Estimate

In this paragraph, we discuss the results in terms of the equivalent CO_2 emission reduction resulting from this blending ratio. The CH_4 and H_2 Global Warming Potentials were applied on the results of the previous calculations to evaluate the equivalent CO_2

emission rates associated with leaks from the natural gas distribution system in both the current natural gas scenario and the 10%vol. H_2 blend scenario. The emission rates of CH_4 and H_2 were converted from standard volume units to mass units, and then, they were multiplied by the respective Global Warming Potential values of both species (CH4 and H_2). This step allowed us to derive average Equivalent CO_2 emission rates for both species. Finally, the average sum of the equivalent CO_2 emission rates was used to evaluate the net environmental benefits (i.e., the greenhouse gas emission reduction) of blending by taking hydrogen losses into account as secondary greenhouse gas emissions. Table 7 shows the mean greenhouse gas emission rates from the natural gas distribution system pipelines and facilities along with the estimated greenhouse gas emission reduction.

Table 7. Greenhouse gas mean emission rates from the natural gas distribution network and emission reduction estimate associated with shifting from natural gas to 10%vol. H_2 blend.

Emission Location	Mean CO_2eq Emission Rate from NG (g/s)	Calculated Mean CO_2eq Emission Rate from Blend (g/s)	CO_2eq Reduction (%)
	Pipeline Type		
Mains	0.40	0.38	5.4
Service Lines	0.09	0.08	7.7
	Pipeline Type and Material		
Mains—Unprotected Steel	0.40	0.37	5.5
Mains—Protected Steel	0.59	0.56	5.2
Mains—Cast Iron	0.44	0.42	5.2
Mains—Plastic	0.14	0.13	6.1
Services—Unprotected Steel	0.17	0.16	6.5
Services—Protected Steel	0.08	0.07	7.2
Services—Cast Iron	0.030	0.027	10.0
Services—Plastic	0.064	0.058	9.4
	Facility Type		
TDTS—Transmission	0.39	0.37	5.5
Metering and Regulating	0.28	0.27	5.5
TDTS—Distribution	0.24	0.22	5.6
Regulating	0.15	0.14	5.8
Vault	0.012	0.011	9.1

Figure 9 compares the emission reduction assessment of CH_4 and the equivalent CO_2 for pipelines and facilities. The difference between the CH_4 reduction and the equivalent CO_2 is attributed to the GWP of H_2 emissions; namely, accounting for H_2 as a secondary greenhouse gas provides more conservative emission reduction estimates.

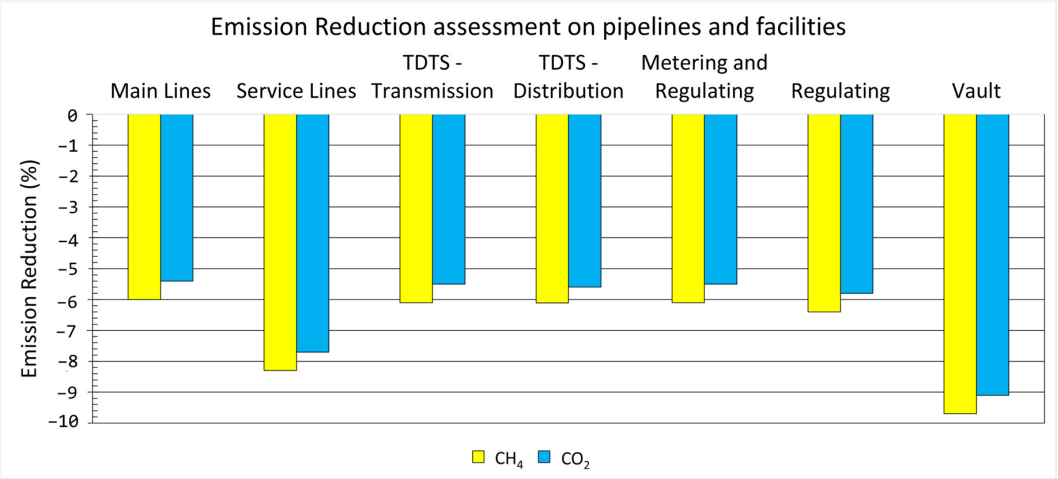

Figure 9. Emission reduction assessment consequential to hydrogen blending into the distribution system and comparison of CH_4 emission reduction versus equivalent CO_2 emission reduction to account for the global warming potential of H_2 leakage.

4. Discussion

This study addresses the change in greenhouse gas emissions from leakages in a natural gas distribution system by converting existing methane emission rate data about localized and measured leaks into theoretical estimates of methane and hydrogen emission rates. The calculation process involves the classification of sampled leaks by the emission rate size and the subsequent mapping of each category into the Re-Kn-Ma domain. The mapping process was used to identify which analytical model describes the flowrate of the leaking gas, and the model was used to calculate the theoretical value of both methane and hydrogen emission rates for each leak in the dataset by re-evaluating the gas properties for a hydrogen–methane blend at 10%vol. H_2. These steps were applied to each leak present in the original dataset to derive a Blended Emissions Dataset of methane and hydrogen emissions. The new dataset was analyzed to evaluate the change in methane emissions from the blend and the hydrogen emissions and the change in total greenhouse gas emissions for each subsystem type compared to the natural gas scenario from which the original dataset was generated.

Our results indicate that converting an existing natural gas network to a low hydrogen–methane blend leads to an increase in the total volumetric leak rate; however, methane-specific emissions decrease, with the increase in gas volume attributed to hydrogen. This behavior highlights the non-uniform change in emission rates across the complex gas network, where flow regimes and conditions vary depending on the leak sources.

For instance, components with low emission rates in a 100% methane scenario tend to experience smaller increases in leak rates compared to those with higher losses. In this regard, Table 3 provides further information about these phenomena. The fluid regime plays a critical role in these dynamics: methane emissions are more significantly reduced under conditions involving a turbulence regime occurring in wider gaps with sonic or near-sonic behavior, where emissions are about 95% of their original value (CF = 1.05 and a CH_4 concentration ratio of 0.9). In contrast, under laminar conditions and a narrower gap and being far from the sonic curve, methane emissions decrease to approximately 90% of their original value (CF = 1 and a CH_4 concentration ratio of 0.9). Hydrogen emissions, however, are more sensitive to rarefaction effects, particularly in regimes described accurately by the free molecular flow model, where hydrogen constitutes 35% of the leak, resulting in 32% of the original methane leak.

These outcomes align with the known properties of gases: smaller, lighter molecules like hydrogen are more likely to escape through narrow gaps, while emissions of larger, heavier molecules, like methane, are more influenced by turbulence and larger gaps. Interestingly, it appears that turbulence does not significantly affect hydrogen emissions at the investigated blending ratio, where the properties of the blend are still dominated by the high methane concentration. This suggests that at low blending ratios, molecular size and weight are less critical in determining leak rates. However, at higher blending ratios or with a 100% hydrogen blend, turbulence could significantly increase hydrogen losses compared to regimes dominated by the continuous laminar flow model, as previously indicated by Schefer et al. [40].

Additionally, the similarity in hydrogen–methane ratios observed in slip flow and continuous Hagen–Poiseuille models [36] suggests that hydrogen selectivity might become prominent in the transition region ($0.1 < Kn < 10$), consistent with experimental observations [23,24,46] in gas separation through capillary tubes [46]. The resulting conversion factors might be conservative, as real-world leakage in such conditions often exhibits higher tortuosity, potentially leading to lower actual emission rates compared to the models' predicted ones [24].

The application of this methodology to a real gas network leakage dataset enabled the quantification of expected methane emission reduction and hydrogen emission rates, facilitating a more accurate assessment of the net environmental impact assessment on both gases. Considering hydrogen as a secondary greenhouse gas affects the overall greenhouse emission estimate, which, in turn, slightly reduces the perceived environmental benefits of

hydrogen blending. This is evident from the CH_4 and equivalent CO_2 emission reduction shown in Figure 9.

In terms of safety, our findings show that hydrogen emissions are highest from bare steel and cast iron mains, while service lines and vaulted facilities exhibit lower emission rates. Given that TDTS systems are located far from sensitive targets, the mainline subsystem in urban areas, often situated under streets, poses greater risks due to its proximity to homes and other vulnerable sites, such as hospitals and schools. Therefore, hydrogen blending strategies should be carefully designed to minimize the risk of hydrogen emissions near sensitive areas. For instance, hydrogen could be blended at specific points and distributed via mainlines, with extraction limited to dedicated end-users, thereby preventing hydrogen from reaching subsystems near residential areas.

Notably, while these emissions reflect the impact of hydrogen blending on the emission rate per single leak event, it is essential to consider that metallic pipelines are sensitive to hydrogen embrittlement. This phenomenon, which becomes more severe at higher blending ratios and high pipeline pressure, can lead to structural damage over time, affecting both the number and the characteristics of leak events in the pipeline system [9,51]. However, this study focuses solely on distribution pipelines, which are operated at significantly lower pressures than transmission ones and have a low ratio (10% vol.). For this reason, we assumed that the leak geometry characteristics remain constant, allowing for a more straightforward analysis of emission rates and leaving the potential complexities introduced by embrittlement outside of the scope of this article.

This methodology could be instrumental in supporting academic and industrial research by applying it to existing leak detection, sampling, and repair databases. Such an approach would allow for the assessment of future losses in natural gas distribution networks before hydrogen is actually injected into the systems. Future experimental research should focus on deepening the understanding of leak dynamics and further refining the mapping between natural gas distribution system failure modes and flow regimes. Additionally, exploring the effect of tortuosity on leak rates and investigating leak geometries could lead to a more accurate calibration of conversion factors.

5. Conclusions

This study presents a novel methodology for estimating emission rates in natural gas networks during a transition to a 10% hydrogen blend by combining established analytical models with direct methane leakage measurements. This methodology was tested on open-source data from Ref. [29], but it can be applied to more recent data collected on existing networks. Furthermore, the authors believe that the application of this methodology on more recent data with a higher degree of detail compared with that of the open-source ones could further improve the evaluation of the emission rate conversion factors, thus, resulting in more accurate estimates of methane and hydrogen emission rates in blending scenarios. Our findings reveal that the total volumetric leak rate increases due to the presence of hydrogen. The increase in gas volume lost is primarily attributed to hydrogen, reflecting the distinct behaviors of methane and hydrogen under varying flow regimes.

Our findings reveal that while the overall volumetric emission rates increase, primarily due to hydrogen's lower density, methane emissions decrease by 5.9% in mainlines and 8.2% in service lines. However, when accounting for the 10% hydrogen blend's effect on the Global Warming Potential, the net reduction in greenhouse gas emissions is 5.4% for mainlines and 7.7% for service lines. Our findings highlight that emission rate changes are not uniform across the network; different components are affected to varying degrees depending on their initial emission rates and the prevailing flow conditions. Methane emissions, for example, are particularly influenced by the fluid regime, with turbulent conditions having a significant impact. In contrast, hydrogen emissions are more sensitive to rarefaction effects, especially in free molecular flow scenarios. Additionally, when hydrogen is treated as a secondary greenhouse gas, the overall reduction in greenhouse gas emissions is less than the results achieved with methane alone. This highlights the

importance of conducting a comprehensive environmental impact assessment to fully understand the implications of hydrogen blending.

In terms of safety, this study identifies specific infrastructure components, such as bare steel and cast iron mains, as more prone to higher hydrogen emissions. The findings suggest that hydrogen blending strategies should be carefully tailored to minimize risks, particularly in urban areas where mainlines are located near sensitive targets.

The methodology developed in this study offers a valuable tool for evaluating the impact of hydrogen blending on emissions in natural gas networks. It can be applied to existing leak detection and repair databases, providing critical insights before the actual deployment of hydrogen in these systems.

Future research should focus on refining the understanding of leak dynamics and improving the accuracy of emission estimates, particularly in relation to the effects of tortuosity and leak geometries.

Supplementary Materials: The following supporting information can be downloaded at: https://www.mdpi.com/article/10.3390/en17246369/s1, Figure S1–S7: Figure S1: Slip-flow correction factor dependency on the Knudsen Number for low pressure infrastructure ($\beta = 1.04$). The variation of this correction factor across the slip-flow regime ($0.01 < Kn < 0.1$) is within 1%; out of conservative reasoning, the value used in this study it is calculated based on the highest Knudsen Number to avoid underestimation of the leak rate. Figure S2: Slip Flow correction factor ratio between Natural Gas and Blend: sensitivity analysis at pressure ratios varying from 1.01 to 4.0. Figure S3: Distribution of the Correction Factor relative change at pressure ratios ranging from 1.01 to 4.03 with uniform step of 0.03. $\beta = 1.04$ is taken as reference case. Higher pressure ratios translate into lower conversion factors. Figure S4: Relative contribution of CH_4 and H_2 mean emission rates from leakage in mains and services. Natural Gas versus blend comparison. Figure S5: Relative contribution of CH_4 and H_2 to the mean emission rates from leakage by pipeline material type. Natural Gas versus blending comparison. Figure S6: Relative contribution of CH_4 and H_2 to the mean emission rates from leakage by Distribution Network Subsystem type. Natural Gas versus blending comparison. Figure S7: Relative contribution of CH_4 and H_2 to the mean emission rates from leakage by component type from Facilities. Natural Gas versus blending comparison.; Table S1: Mean CH_4 and H_2 emission rate values for each recorded component in facilities.

Author Contributions: Conceptualization, R.P.; methodology, R.P.; validation, R.P. and F.D.M.; formal analysis, R.P.; investigation, R.P.; resources, R.P.; data curation, R.P.; writing—original draft preparation, R.P.; writing—review and editing, R.P., F.D.M. and A.L.; visualization, R.P. and F.D.M.; supervision, F.D.M. and A.L.; project administration, A.L.; funding acquisition, A.L. All authors have read and agreed to the published version of the manuscript.

Funding: F.D. Minuto carried out this study within Ministerial Decree no. 1062/2021 and received funding from the FSE REACT-EU-PON Ricerca e Innovazione, 2014–2020. R. Paglini carried out this study within Ministerial Decree no. 1061/2021 and received funding from the FSE REACT-EU-PON Ricerca e Innovazione, 2014–2020.

Data Availability Statement: The data presented in this study are available in Lamb B.K, et al. (Appendix E) [29].

Acknowledgments: This research was conducted without any external support beyond the efforts of the authors.

Conflicts of Interest: The authors declare no conflicts of interest. The funders had no role in the design of the study; in the collection, analyses, or interpretation of data; in the writing of the manuscript; or in the decision to publish the results.

References

1. Intergovernmental Panel on Climate Change the Earth's Energy Budget, Climate Feedbacks and Climate Sensitivity. In *Climate Change 2021–The Physical Science Basis*; Cambridge University Press: Cambridge, UK, 2023; pp. 923–1054.
2. Fox, T.A.; Barchyn, T.E.; Risk, D.; Ravikumar, A.P.; Hugenholtz, C.H. A Review of Close-Range and Screening Technologies for Mitigating Fugitive Methane Emissions in Upstream Oil and Gas Erratum: A Review of Close-Range and Screening Technologies for Mitigating Fugitive Methane Emissions in Upstream Oil and Gas. *Environ. Res. Lett.* **2019**, *14*, 053002. [CrossRef]
3. Fox, T.A.; Hugenholtz, C.H.; Barchyn, T.E.; Gough, T.R.; Gao, M.; Staples, M. Can New Mobile Technologies Enable Fugitive Methane Reductions from the Oil and Gas Industry? *Environ. Res. Lett.* **2021**, *16*, 064077. [CrossRef]
4. United Nations Environment Programme (UNEP). *Mineral Methane Initiative OGMP2.0 Framework*; United Nations Environment Programme (UNEP): Nairobi, Kenya, 2020.
5. United Nations Environmental Programme (UNEP). *Guidance Document: Reconciliation and Uncertainty (U&R) in Methane Emissions Estimates for OGMP2.0*; United Nations Environment Programme (UNEP): Nairobi, Kenya, 2022.
6. Ekhtiari, A.; Flynn, D.; Syron, E. Green Hydrogen Blends with Natural Gas and Its Impact on the Gas Network. *Hydrogen* **2022**, *3*, 402–417. [CrossRef]
7. Baird, A.R.; Glover, A.M.; Ehrhart, B.D. *Sandia Report Review of Release Behavior of Hydrogen & Natural Gas Blends from Pipelines*; Sandia National Laboratories: Albuquerque, New Mexico, 2021.
8. Mahajan, D.; Tan, K.; Venkatesh, T.; Kileti, P.; Clayton, C.R. Hydrogen Blending in Gas Pipeline Networks—A Review. *Energies* **2022**, *15*, 3582. [CrossRef]
9. Erdener, B.C.; Sergi, B.; Guerra, O.J.; Lazaro Chueca, A.; Pambour, K.; Brancucci, C.; Hodge, B.M. A Review of Technical and Regulatory Limits for Hydrogen Blending in Natural Gas Pipelines. *Int. J. Hydrogen Energy* **2023**, *48*, 5595–5617. [CrossRef]
10. Florisson, O.; Huizing, R. A Practical Step towards "Hydrogen": The Conditions under Which the Existing Natural Gas System Can Be Used for Mixtures of Hydrogen and Natural Gas (the NATURALHY-Project). In Proceedings of the International Gas Research Conference, Vancouver, BC, Canada, 1–4 November 2004.
11. Florisson, O.; Lowesmith, B.; Hankinson, G. The Value of the Existing Natural Gas System for Hydrogen, the Sustainable Future Energy Carrier (Progress Obtained in the Naturalhy-Project). 23rd World Gas Conference, Amsterdam. 2006. Available online: http://members.igu.org/html/wgc2006/pdf/paper/add11415.pdf (accessed on 4 April 2023).
12. Alliat, I.; Heerings, J. Assessing the Durability and Integrity of Natural Gas Infrastructures for Transporting and Distributing Mixtures of Hydrogen and Natural Gas. 2005. Available online: https://h2tools.org/sites/default/files/2019-08/230120.pdf (accessed on 4 April 2023).
13. Florisson, O.; Huizing, R.R. The Safe Use of the Existing Natural Gas System for Hydrogen (Overview of the NATURALHY-Project). 2005. Available online: https://h2tools.org/sites/default/files/2019-09/The%20Safe%20Use%20of%20the%20Existing%20Natural%20Gas%20System%20for%20Hydrogen%20(Overview%20of%20the%20Naturalhy-Project).pdf. (accessed on 4 April 2023).
14. Melaina, M.W.; Antonia, O.; Penev, M. *Blending Hydrogen into Natural Gas Pipeline Networks: A Review of Key Issues*; National Renewable Energy Laboratory (NREL): Golden, CO, USA, 2013. [CrossRef]
15. NATURALHY-GERG. Available online: https://www.gerg.eu/projects/hydrogen/naturalhy/ (accessed on 11 July 2023).
16. Lowesmith, B.J.; Hankinson, G.; Spataru, C.; Stobbart, M. Gas Build-up in a Domestic Property Following Releases of Methane/Hydrogen Mixtures. *Int. J. Hydrogen Energy* **2009**, *34*, 5932–5939. [CrossRef]
17. Wooley, R.M.; Fairweather, M.; Falle, S.A.E.G.; Giddings, J.R. Predictions of the Consequences of Natural Gas-Hydrogen Explosions Using a Novel CFD Approach. *Comput. Aided Chem. Eng.* **2008**, *25*, 919–924. [CrossRef]
18. Bu, F.; He, Y.; Lu, Q.; Liu, M.; Bai, J.; Lv, Z.; Leng, C. Analysis of Leakage and Diffusion Characteristics and Hazard Range Determination of Buried Hydrogen-Blended Natural Gas Pipeline Based on CFD. *ACS Omega* **2024**, *9*, 39202–39218. [CrossRef]
19. Su, Y.; Li, J.; Yu, B.; Zhao, Y. Numerical Investigation on the Leakage and Diffusion Characteristics of Hydrogen-Blended Natural Gas in a Domestic Kitchen. *Renew. Energy* **2022**, *189*, 899–916. [CrossRef]
20. Li, H.; Cao, X.; Du, H.; Teng, L.; Shao, Y.; Bian, J. Numerical Simulation of Leakage and Diffusion Distribution of Natural Gas and Hydrogen Mixtures in a Closed Container. *Int. J. Hydrogen Energy* **2022**, *47*, 35928–35939. [CrossRef]
21. Sand, M.; Skeie, R.B.; Sandstad, M.; Krishnan, S.; Myhre, G.; Bryant, H.; Derwent, R.; Hauglustaine, D.; Paulot, F.; Prather, M.; et al. A Multi-Model Assessment of the Global Warming Potential of Hydrogen. *Commun. Earth Environ.* **2023**, *4*, 203. [CrossRef]
22. Log, T.; Pedersen, W.B. A Common Risk Classification Concept for Safety Related Gas Leaks and Fugitive Emissions? *Energies* **2019**, *12*, 4063. [CrossRef]
23. Nohora, M.; Mejia, H.; Brouwer, J. Gaseous fuel leakage from natural gas infrastructure. In Proceedings of the ASME 2018 International Mechanical Engineering Congress and Exposition, Pittsburgh, PA, USA, 9–15 November 2018.
24. Hormaza Mejia, A.; Brouwer, J.; Mac Kinnon, M. Hydrogen Leaks at the Same Rate as Natural Gas in Typical Low-Pressure Gas Infrastructure. *Int. J. Hydrog. Energy* **2020**, *45*, 8810–8826. [CrossRef]
25. Qin, C.; Tian, Y.; Yang, Z.; Hao, D.; Feng, L. Quantitative Analysis of Hydrogen Leakage Flow Measurement and Calculation in the On-Board Hydrogen System Pipelines. *Int. J. Hydrogen Energy* **2024**, *89*, 1025–1039. [CrossRef]
26. Cooper, J.; Dubey, L.; Bakkaloglu, S.; Hawkes, A. Hydrogen Emissions from the Hydrogen Value Chain-Emissions Profile and Impact to Global Warming. *Sci. Total Environ.* **2022**, *830*, 154624. [CrossRef]

27. Zavala-Araiza, D.; Lyon, D.R.; Alvarez, R.A.; Davis, K.J.; Harriss, R.; Herndon, S.C.; Karion, A.; Kort, E.A.; Lamb, B.K.; Lan, X.; et al. Reconciling Divergent Estimates of Oil and Gas Methane Emissions. *Proc. Natl. Acad. Sci. USA* **2015**, *112*, 15597–15602. [CrossRef]
28. Alvarez, R.A.; Zavala-Araiza, D.; Lyon, D.R.; Allen, D.T.; Barkley, Z.R.; Brandt, A.R.; Davis, K.J.; Herndon, S.C.; Jacob, D.J.; Karion, A.; et al. Assessment of Methane Emissions from the U.S. Oil and Gas Supply Chain. *Science* **2018**, *361*, 186–188. [CrossRef]
29. Lamb, B.K.; Edburg, S.L.; Ferrara, T.W.; Howard, T.; Harrison, M.R.; Kolb, C.E.; Townsend-Small, A.; Dyck, W.; Possolo, A.; Whetstone, J.R. Direct Measurements Show Decreasing Methane Emissions from Natural Gas Local Distribution Systems in the United States. *Environ. Sci. Technol.* **2015**, *49*, 5161–5169. [CrossRef]
30. Weller, Z.D.; Roscioli, J.R.; Conner Daube, W.; Lamb, B.K.; Ferrara, T.W.; Brewer, P.E.; Von Fischer, J.C. Vehicle-Based Methane Surveys for Finding Natural Gas Leaks and Estimating Their Size: Validation and Uncertainty. *Environ. Sci. Technol.* **2018**, *52*, 11922–11930. [CrossRef]
31. Weller, Z.D.; Hamburg, S.P.; Von Fischer, J.C. A National Estimate of Methane Leakage from Pipeline Mains in Natural Gas Local Distribution Systems. *Environ. Sci. Technol.* **2020**, *54*, 8967. [CrossRef]
32. Jolly, P.; Marchand, L. Leakage Predictions for Static Gasket Based on the Porous Media Theory. *J. Press. Vessel. Technol.* **2009**, *131*, 021203. [CrossRef]
33. Grine, L.; Bouzid, A.H. Correlation of Gaseous Mass Leak Rates through Micro- and Nanoporous Gaskets. *J. Press. Vessel. Technol. Trans. ASME* **2011**, *133*, 021402. [CrossRef]
34. Kazeminia, M.; Bouzid, A.-H. Prediction of leak rates in porous braided packing rings. In Proceedings of the ASME 2015 Pressure Vessels and Piping Conference, Boston, MA, USA, 19–23 July 2015.
35. Kazeminia, M.; Bouzid, A.H. Leak Prediction through Porous Compressed Packing Rings: A Comparison Study. *Int. J. Press. Vessel. Pip.* **2018**, *166*, 1–8. [CrossRef]
36. Munson, B.R.; Okiishi, T.H.; Rothmayer, A.P.; Huebsch, W.W. *Fundamentals of Fluid Mechanics*, 7th ed.; John Wiley & Sons, Inc.: Jefferson City, MO, USA, 2012; ISBN 9781118214596.
37. Kast, W.; Hohenthanner, C.R. Mass Transfer within the Gas-Phase of Porous Media. *Int. J. Heat. Mass. Transf.* **2000**, *43*, 807–823. [CrossRef]
38. van den Bosch, C.J.H.; Weterings, R.A.P.M.; Duijm, N.J.; Bakkum, E.A.; Mercx, W.P.M.; van den Berg, A.C.; Engelhard, W.F.J.M.; van Doormaal, J.C.A.M.; van Wees, R.M.M. *Methods for the Calculation of Physical Effects Due to Releases of Hazardous Materials (Liquid and Gases)—Yellow Book*; Min. VROM: The Hague, The Netherlands, 2005.
39. Ge, X.; Sutton, W.H. Analysis and Test of Compressed Hydrogen Interface Leakage by Commercial Stainless Steel (NPT) Fittings. *SAE Tech. Pap.* **2006**. [CrossRef]
40. Schefer, R.; Houf, W.; San Marchi, C.; Chernicoff, W.P.; Englom, L. Characterization of Leaks from Compressed Hydrogen Dispensing Systems and Related Components. *Int. J. Hydrogen Energy* **2006**, *31*, 1247–1260. [CrossRef]
41. Kanellopoulos, K.; Busch, S.; De Felice, M.; Giaccaria, S.; Costescu, A. *Blending Hydrogen from Electrolysis into the European Gas Grid*; EUR 30951 EN; Publications Office of the European Union: Luxembourg, 2022; ISBN 978-92-76-46346-7. [CrossRef]
42. Kobayashi, Y.; Kurokawa, A.; Hirata, M. Viscosity Measurement of Hydrogen-Methane Mixed Gas for Future Energy Systems. *J. Therm. Sci. Technol.* **2007**, *2*, 236–244. [CrossRef]
43. Colin, S. Rarefaction and Compressibility Effects on Steady and Transient Gas Flows in Microchannels. *Microfluid. Nanofluidics* **2005**, *1*, 268–279. [CrossRef]
44. Naris, S.; Valougeorgis, D.; Kalempa, D.; Sharipov, F. Flow of Gaseous Mixtures through Rectangular Microchannels Driven by Pressure, Temperature, and Concentration Gradients. *Phys. Fluids* **2005**, *17*, 100607. [CrossRef]
45. Naris, S.; Valougeorgis, D.; Kalempa, D.; Sharipov, F. Gaseous Mixture Flow between Two Parallel Plates in the Whole Range of the Gas Rarefaction. *Phys. A Stat. Mech. Its Appl.* **2004**, *336*, 294–318. [CrossRef]
46. Gao, R.; Sharipov, F.; Liow, J.L. Experimental Investigation of the Separation of Binary Gaseous Mixtures Flowing through a Capillary Tube. *Phys. Fluids* **2020**, *32*, 112008. [CrossRef]
47. Weller, Z.D.; Yang Keun, D.; Von Fischer, J.C. An Open Source Algorithm to Detect Natural Gas Leaks from Mobile Methane Survey Data. *PLoS ONE* **2019**, *14*, e0212287. [CrossRef]
48. D'Zurko, D.; Mallia, J. Measurement Technologies Look to Improve Methane Emissions. *Pipeline Gas. J.* **2018**, *245*. Available online: https://pgjonline.com/magazine/2018/february-2018-vol-245-no-2/features/measurement-technologies-look-to-improve-methane-emissions (accessed on 17 February 2023).
49. MacMullin, S.; Rongère, F.X. Measurement-Based Emissions Assessment and Reduction through Accelerated Detection and Repair of Large Leaks in a Gas Distribution Network. *Atmos. Environ. X* **2023**, *17*, 100201. [CrossRef]
50. Zhu, J.; Pan, J.; Zhang, Y.; Li, Y.; Li, H.; Feng, H.; Chen, D.; Kou, Y.; Yang, R. Leakage and Diffusion Behavior of a Buried Pipeline of Hydrogen-Blended Natural Gas. *Int. J. Hydrogen Energy* **2023**, *48*, 11592–11610. [CrossRef]
51. Sofian, M.; Haq, M.B.; Al Shehri, D.; Rahman, M.M.; Muhammed, N.S. A Review on Hydrogen Blending in Gas Network: Insight into Safety, Corrosion, Embrittlement, Coatings and Liners, and Bibliometric Analysis. *Int. J. Hydrogen Energy* **2024**, *60*, 867–889. [CrossRef]